

X-ray fluctuation timescale and Black Hole mass relation in AGN

Amri Wandel¹ and Mathew Malkan²

¹Racah Institute, The Hebrew University of Jerusalem,
Jerusalem 91904, Israel
email: amri@huji.ac.il

²Dept. of Astronomy, University of California, Los Angeles, California , U.S.A.
email: malkan@astro.ucla.edu

Abstract. We analyze the fluctuations in the X-ray flux of 20 AGN (mainly Seyfert 1 galaxies) monitored by RXTE and XMM-Newton with a sampling frequency ranging from hours to years, using structure function (SF) analysis. We derive SFs over four orders of magnitude in the time domain (0.03-300 days). Most objects show a characteristic time scale, where the SF flattens or changes slope. For 10 objects with published power-spectral density (PSD) the break time scales in the SF and PSD are similar and show a good correlation. We also find a significant correlation between the SF timescale and the mass of the central black hole, determined for most objects by reverberation mapping.

Keywords. AGN, X-ray, Fluctuations, Structure Functions, Power Spectral Density, Black Holes

1. Introduction

The strong, irregular X-ray variability observed in many Seyfert galaxies on timescales as short as hours indicates that these X-rays are emitted from a region close to the central black hole. Doubling time scales were used as the first quantification of variability; characteristic time scales of X-ray variability seemed to correlate with luminosity and black hole mass Wandel & Mushotzky (1986).

For quasi-periodic and stochastic light curves the variability is often characterized through the power spectral density (PSD). The PSD is the variability amplitude per frequency, so it describes the variability power contained within a frequency interval. A similar measure that is sometimes used is the structure function, which describes the variability amplitude as a function of time scale. The variability of quasi-periodic and stochastic light curves may then be characterized by representing the power spectrum in a parametric form. However, irregular sampling or sequences of regular sampling separated by gaps often cause problems in measuring variability features from a light curve, which is the case in all ground-based and often also space-based data. Ideally the variability must be quantified over a broad range of time scales, to maximize the probability of detecting a characteristic variability time scale and to avoid spurious features caused by an insufficiently long observing time.

The Rossi X-ray Timing Explorer (XTE) has been the first mission to provide sustained monitoring on given objects for time scales up to months and years. High dynamic-range X-ray PSDs were published for approximately 10 AGN, (e.g., Edelson & Nandra (1999), Uttley, McHardy & Papadakis (2002), Markowitz *et al.* (2003), Chatterjee *et al.* (2009;2011), Rothschild *et al.* (2011)). Typically they are parameterized as a broken power law; on long timescales the fluctuation power is flat, scaling as a power of f^{0-1} , and on short timescales it is descending more steeply, with slopes of 2-3. The break between

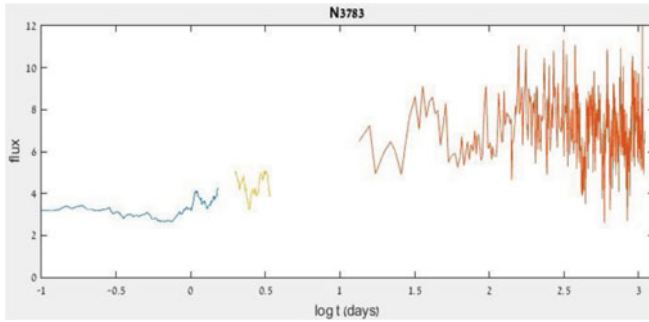


Figure 1. Combined logarithmic light curve of NGC 3783. The X-ray flux vs. $\log(1/\text{frequency})$ in units of days. Shown are the light curves of XTE (right curve) and XMM (the two left curves).

these two regimes is in the range of roughly 10^{4-6} Hz, corresponding to time scales t_{PSD} ranging from a few hours up to weeks.

2. Structure functions

The structure function (SF) measures the mean relative amplitudes of pairs of flux variations as a function of their time difference (Simonetti *et al.* (1985)). While the PSD requires strictly even sampling to compute, the SF can be derived for uneven and gappy sampling. The SF has been applied to optical AGN monitoring data (Webb and Malkan (2000); Collier & Peterson (2001)) as well as to X-ray light curves of blazars. As long as the number/size of gaps are not too large, meaningful results can be obtained; however this procedure is not foolproof, and sampling limitations (especially the lack of long enough timescales) can produce spurious features, as demonstrated by Emmanoulopoulos, McHardy & Uttley (2010) (hereafter E10), who give a detailed analyses of the caveats and cautions for SF measurement and interpretation. Recently a new method - continuous-time autoregressive moving average (CARMA) has been suggested (Kelly *et al.* 2014) to handle irregular sampling and gaps.

We define the amplitude-averaged SF as

$$S(\tau)^2 = \sum_k [f(t_k) - f(t_k - \tau)]^2$$

where $f(t_k)$ is the normalized flux at time point t_k . As advised in E10, we work with the $\log f$ - \log SF. Typically, the fluctuation amplitude is increasing with time difference, as larger fluctuations are present on longer timescales.

To derive errors on each SF bin, we used two methods. The first is an enhanced χ^2 method (Collier & Peterson (2001)). The statistical uncertainties in structure functions are defined by $\sigma_i / (N_i/2)^{1/2}$ where σ_i is the root mean square (rms) deviations about the mean structure function value in bin i and N_i is the number of pairs of data points in the i -th bin. This ad hoc, but reasonable, error estimates reflect the fact that not all pairs of measurements in a given bin are independent. The second method, which for sparser sampling gives more realistic errors for light curves, is a Monte Carlo procedure (e.g., Kataoka *et al.* (2001) and E10).

For each light curve/SF segment we assume a form for the underlying PSD (using the published PSD parameters if they exist; otherwise we make a PSD analyses with the incomplete data and use the resulting power law (Emmanoulopoulos, private communication). For each curve segment, we simulate 100 light curves using the algorithm of Timmer & Koenig (1995), re-sample them in the same manner as the observed light

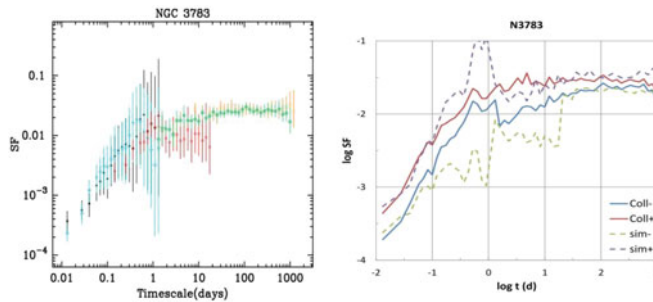


Figure 2. Combined $\log(\text{SF})$ - $\log t$ diagram for NGC 3783. Upper and lower error limits, calculated for the 95%-th percentile with both methods, MC simulations (dashed) and Collier & Peterson (2001) (solid).

curve, and measured the SF. This yields relatively larger errors towards longer time scales, which reflects systematic uncertainties in the SF introduced by red-noise leak and/or by gaps in the sampling. We adopt the 95% confidence errors on each binned SF point, as a trade-off between 1σ errors for χ^2 -fitting and a higher confidence level, that would reflect more closely the systematic SF behavior for each time scale bin. Finally we combine the $\log(\text{SF})$ - $\log t$ diagrams for all data segments for each object to produce a combined SF over a broad range of timescales.

Similar SF figs of have been obtained for NGC 3516, 4051, 4151, 5584, 7469, IC4329a, MCG 6-30-15, Fairall 9, Mkn 766. The two last ones do not show an obvious break (Wandel, Markowitz and Malkan, in preparation). Comparing χ^2 -fits of the SF to an unbroken power-law and a broken one, we find that for almost all objects with a full range time series (4 orders of magnitude in temporal range) data sources, the improvement in a χ^2 fit when including a break is statistically significant. It is important though to caution that the SF points are not all independent, and unlike the Monte Carlo method applied to PSDs, this method also does not take into account distortion effects such as aliasing or red-noise leak, which could introduce scatter into the determination of the break point t_{SF} .

3. The SF-break timescale and the Black Hole mass relation

It can be shown that for good enough data the PSD and SF power-law slopes are related: when the sampling is of sufficient quality and dynamic range the slope of $\text{PSD}(\nu)$ minus one equals the slope of $\text{SF}(\tau)$ (E10, appendix A). If a change in power-law slope exists in the broadband PSD, we should expect to find a change in power-law slope in the broadband SF at a similar time scale. Comparing the SF and the PSD timescales for the objects with published PSD, it appears that a distinct break in the SF corresponds to the break in the PSD.

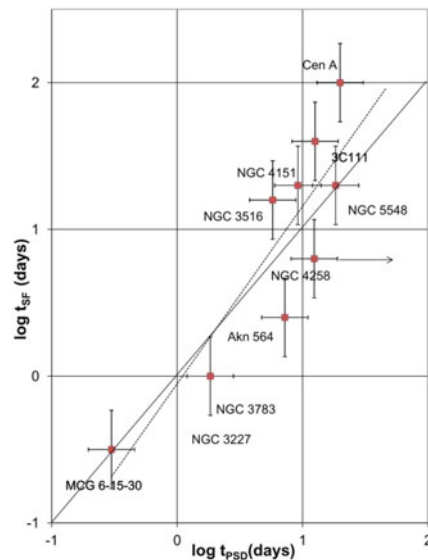


Figure 3. The time scale corresponding to the SF break vs. that of the break in the PSD. The best fit has a slope of 1. Solid line denotes equality, dashed line is the best fit. Typical errors are denoted by the crosses; the vertical error bars would be larger for a higher confidence level.

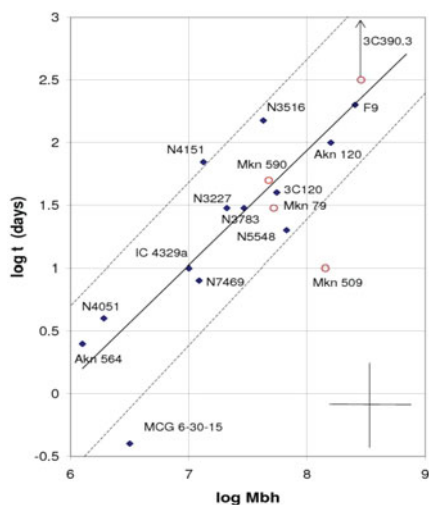


Figure 4. SF break time vs. black hole mass for 13 Seyfert galaxies. Four more objects with weak breaks are denoted by circles. The solid line is the best linear fit, dashed lines are linear extrapolations of the two breaks in the PSD of Cyg X-1. Typical errors are denoted by the cross in the lower right.

We find a similar relation between the SF break timescale and the BH mass (fig. 3). The black hole masses of most of the Seyferts are estimated by reverberation mapping (Peterson *et al.* 2004). For Akn 564, 3C111 and MCG 6-15-30, which do not have reverberation data, single-epoch H β is used with the empirical L-R relation (Wandel, Peterson & Malkan 1999; (Kaspi *et al.* 2000)). We note that the timescale of the SF-break is strongly correlated with the black hole mass, the best fit being consistent with a linear relation, $M_{\text{BH}} = 1.010^6 (\tau_{\text{SF}}/\text{day})$. Almost all points coincide, within the errors, with the extrapolated "Cyg-X1 line" marked by the dashed diagonal lines in fig. 3, which shows the extrapolation from the break time - M_{BH} relation for the two breaks in the PSD of Cyg X-1, corresponding to 0.2 sec and 5 sec, respectively. This results is consistent with similar trend found in AGN between the black hole mass and the break time in the PSD.

We acknowledge a long lasting collaboration with Alex Markowitz. AW acknowledges the hospitality of the Physics and Astronomy department at UCLA.

References

- Chatterjee *et al.* 2009, *ApJ* 704, 1689
 Chatterjee *et al.* 2011, *ApJ* 734, 43
 Collier, S. & Peterson, B. 2001, *ApJ* 2001,555, 775
 Edelson, R. & Nandra, K. 1999, *ApJ* 514, 682
 Emmanoulopoulos, D., & McHardy, I. M. and Uttley, P. 2010, *MNRAS* 404, 931
 Kaspi, S. *et al.* 2000, *ApJ* 533, 631
 Kataoka *et al.* . 2001, *ApJ* 560, 659
 Kelly, B. C. *et al.* 2014, *ApJ* 788, 33
 Markowitz *et al.* 2003, *ApJ* 593, 96
 McHardy *et al.* 2005, *MNRAS* 348, 783
 McHardy, I. M. *et al.* 2006, *Nature* 444 730
 Peterson, B. *et al.* 2004, *ApJ* 613, 632
 Rothschild, R. E., *et al.* 2011, *ApJ* 733, 23
 Simonetti *et al.*. 1985, *ApJ* 295, 46S
 Timmer & Koenig 1995, *A & A* 300, 707
 Uttley, P., McHardy, I. M. & Papadakis 2002, *MNRAS* 332,231
 Uttley, P. & McHardy, I. M. 2005, *MNRAS* 363,586
 Wandel, A. & Mushotzky, R. F. 1986, *ApJ* 306, L61
 Wandel, A., Peterson, B. & Malkan, M. 1999, *ApJ* 526, 579
 Webb, W. & Malkan, M. 2000, *ApJ* 540, 652

The PSD timescales scale approximately linearly with the estimated black hole mass (McHardy *et al.* (2006); Uttley and McHardy (2005)). Using the structure function method enables us to include also objects which do not have sufficient sampling for constructing a PSD. Altogether we have 17 objects. We find a similar relation between the SF break timescale and the BH mass (fig. 3). The black hole masses of most of the Seyferts are estimated by reverberation mapping (Peterson *et al.* 2004). For Akn 564, 3C111 and MCG 6-15-30, which do not have reverberation data, single-epoch H β is used with the empirical L-R relation (Wandel, Peterson & Malkan 1999; (Kaspi *et al.* 2000)). We note that the timescale of the SF-break is strongly correlated with the black hole mass, the best fit being consistent with a linear relation, $M_{\text{BH}} = 1.010^6 (\tau_{\text{SF}}/\text{day})$. Almost all points coincide, within the errors, with the extrapolated "Cyg-X1 line" marked by the dashed diagonal lines in fig. 3, which shows the extrapolation from the break time - M_{BH} relation for the two breaks in the PSD of Cyg X-1, corresponding to 0.2 sec and 5 sec, respectively. This results is consistent with similar trend found in AGN between the black hole mass and the break time in the PSD.